

Interplay between magnetism and superconductivity in UTe₂Di S. Wei,^{1,2,3} David Saykin,^{1,4,3} Oliver Y. Miller[Ⓞ],^{1,4} Sheng Ran,^{5,6,7} Shanta R. Saha,⁵ Daniel F. Agterberg,⁸ Jörg Schmalian,⁹ Nicholas P. Butch,^{5,6} Johnpierre Paglione,^{5,6,10} and Aharon Kapitulnik[Ⓞ]^{1,2,3,4}¹*Geballe Laboratory for Advanced Materials, Stanford University, Stanford, California 94305, USA*²*Department of Applied Physics, Stanford University, Stanford, California 94305, USA*³*Stanford Institute for Materials and Energy Sciences, SLAC National Accelerator Laboratory, 2575 Sand Hill Road, Menlo Park, California 94025, USA*⁴*Department of Physics, Stanford University, Stanford, California 94305, USA*⁵*Department of Physics, Quantum Materials Center, University of Maryland, College Park, Maryland 20742, USA*⁶*NIST Center for Neutron Research, National Institute of Standards and Technology, Gaithersburg, Maryland 20899, USA*⁷*Department of Physics, Washington University in St. Louis, St. Louis, Missouri 63130, USA*⁸*Department of Physics, University of Wisconsin-Milwaukee, Milwaukee, Wisconsin 53201, USA*⁹*Institute for Quantum Materials and Technologies, Karlsruhe Institute of Technology, Karlsruhe 76021, Germany*¹⁰*The Canadian Institute for Advanced Research, Toronto, Ontario, Canada M5G 1M1*

(Received 1 September 2021; revised 24 November 2021; accepted 10 January 2022; published 26 January 2022)

Time-reversal symmetry breaking (TRSB) in UTe₂ was inferred from observations of a spontaneous Kerr response in the superconducting state after cooling in zero magnetic field, while a finite *c*-axis magnetic field training was further used to determine the nature of the nonunitary composite order parameter of this material. Here, we present an extensive study of the magnetic-field-trained Kerr effect, which unveils a unique critical state of pinned “ferromagnetic vortices.” We show that a remanent Kerr signal appears following the removal of a training magnetic field, which reflects the response to the TRSB order parameter and the external magnetic field through the paramagnetic susceptibility. This unambiguously demonstrates the importance of the magnetic fluctuations and their intimate relation to the composite order parameter. Focusing the beam on the center of the sample, we are able to accurately determine the maximum field that is screened by the critical state and the respective critical current. Measurements in the presence of magnetic field show the tendency of the superconductor to produce shielding currents that oppose the increase in vortex-induced magnetization due to the diverging paramagnetic susceptibility.

DOI: [10.1103/PhysRevB.105.024521](https://doi.org/10.1103/PhysRevB.105.024521)**I. INTRODUCTION**

UTe₂ is an example of superconductivity in the presence of magnetic fluctuations that persist to temperatures approaching zero, suggesting a magnetic quantum critical phenomenon. The observations of two successive superconducting transitions in specific heat and the spontaneous polar Kerr effect (PKE) [1] along the crystallographic *c* axis led to the conclusion that superconductivity in UTe₂ is characterized by a two-component order parameter that breaks time-reversal symmetry [1–3]. These conclusions follow from measurements on samples that show two transitions at ambient pressure. While recent reports found that some samples show only one transition at ambient pressure, leading to the suggestion that two transitions might have an extrinsic origin [4,5], the observation of a Kerr effect that has its onset near *T_c* suggests that this is not the case, and the associated time-reversal symmetry breaking (TRSB) is intimately related to the superconducting state of these samples. Within the several possibilities considered for the symmetry representation, the one that seemed to agree with the data was ($\psi_1 \in B_{3u}$, $\psi_2 \in B_{2u}$) [1,3], implying a nonunitary order parameter, which we previously argued can be stabilized by magnetic fluctuations [1].

However, the nature of these magnetic fluctuations is still not fully understood. Initial considerations based on extrapolation from other similar uranium-based superconductors including URhGe, UCoGe, and UGe₂ strongly support a spin-triplet state mediated by ferromagnetic fluctuations [1–3]. This is also supported by nuclear magnetic resonance (NMR) studies, which reveal the emergence of magnetic fluctuations along the *a* axis below ~ 20 K [6], and strong support for spin-triplet pairing through analysis of the anisotropy of the spin susceptibility [7]. Muon-spin relaxation experiments indicate coexistence of ferromagnetic fluctuations and superconductivity, where the temperature dependence of the dynamic relaxation rate down to 0.4 K agrees with the self-consistent renormalization theory of spin fluctuations for a three-dimensional weak itinerant ferromagnetic metal [8]. Magnetization measurements can be collapsed onto a single curve using a theory of metallic ferromagnetic quantum criticality [9], strongly suggesting a zero-temperature ferromagnetic transition. However, recent neutron scattering results show that magnetic fluctuations in UTe₂ are dominated by incommensurate spin fluctuations near an antiferromagnetic ordering wave vector and extend to at least 2.6 meV,

suggesting that these fluctuations play an important role in the development of the superconducting state [10,11]. Furthermore, recent transport and thermodynamics studies under hydrostatic pressure suggest that the superconducting transition temperature is maximized near a putative anti-ferromagnetic quantum critical point occurring at a modest pressure of ~ 1.3 GPa [12]. While two superconducting states have been confirmed in these experiments, the nature of the magnetic interaction associated with each of the states could be different [5,12]. Focusing on the superconducting state at ambient pressure, one way to resolve the magnetic nature of the superconducting state of UTe_2 is to test what magnetic state the superconducting order parameter nucleates upon interaction with the magnetic fluctuations in both the Meissner and vortex states.

While the TRSB property could be determined unambiguously from the observation of the spontaneous Kerr response in the superconducting state after cooling in zero magnetic field, understanding the field-cool data requires more attention. First, the strong ferromagnetic fluctuations at low temperatures may counter the onset of Meissner currents. In addition, indications are that UTe_2 exhibits very strong pinning effects [13]. For example, removing the magnetic field at low temperatures after a field cool may result in a finite remanent magnetization due to trapped flux [14], which interacts with the fluctuating magnetic moments as well as with the TRSB superconductor [1]. Such a behavior would be enhanced when the material is cooled above the lower critical field, H_{c1} , and a critical-state concept is expected to be applicable [15,16]. In this case the Kerr effect will be an ideal probe of the local magnetization, particularly aiming at the center of the sample's surface perpendicular to the applied magnetic field.

In this paper we report on high-resolution polar Kerr effect measurements of single-crystal UTe_2 samples under various conditions involving combinations of field cool (FC), zero-field cool (ZFC), field warmup (FW), and zero-field warmup (ZFW). The assemblage of our results suggest strong correlations between the time-reversal symmetry breaking order parameter, the ferromagnetic susceptibility, and the external magnetic field—when applied. First, as previously reported [1], the observation of a finite Kerr response under ZFW conditions that followed ZFC unambiguously prove the time-reversal symmetry breaking of the superconducting order parameter. The varying magnitude of the effect (with a maximum amplitude of $\sim 0.4 \mu\text{rad}$) and its random sign observed under those conditions is expected from a spontaneous symmetry breaking effect that exhibits twofold domains. Furthermore, ZFW measurements that followed a finite FC schedule show a low-temperature, field-independent Kerr response of $\sim 0.4 \mu\text{rad}$ when the cooling field is $\lesssim 30$ Oe and an increasing low-temperature Kerr response for larger cooling magnetic fields. This remanent Kerr response, which originates from a combination of remanent magnetization associated with trapped vortices and the superconducting order parameter, extrapolates to saturate at $H^* \sim 920$ Oe. The above behavior, as well as the temperature dependence of the remanent Kerr effect, particularly the way it vanishes near T_c , suggests an unusual interplay between magnetism and the TRSB order parameter in a nonunitary superconductor.

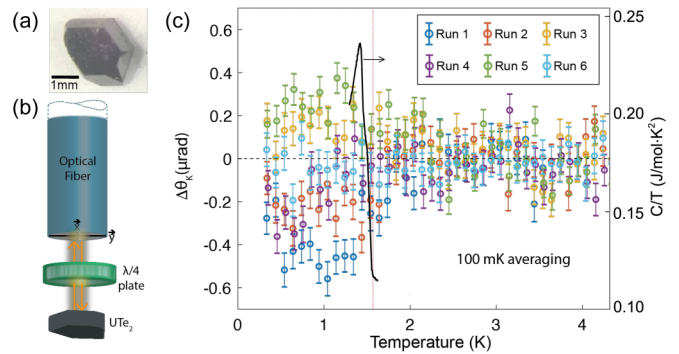


FIG. 1. (a) Crystal used for Kerr measurements. (b) End part of the apparatus (for full description, see SM [17]). (c) Five different zero-field-cool Kerr data for a superconducting UTe_2 with $T_c \approx 1.55$ K. The solid line is the specific heat, C/T , in the temperature range of the transition (1.3–1.65 K) of a same-batch sample, showing the double transition [1].

Our observation that the TRSB in UTe_2 can be trained by a magnetic field along the crystallographic c axis (coinciding with the z direction in our notation) requires the presence of a term $\sim H_z i(\psi_1 \psi_2^* - \psi_1^* \psi_2) \equiv H \tilde{\psi}$. Hence $\tilde{\psi}$ is a TRSB composite order parameter. A resulting c -axis magnetization will yield the following contribution to the free energy:

$$f_m = \alpha m^2 + \gamma m \tilde{\psi} - mH. \quad (1)$$

Since the Curie temperature is suppressed to $T = 0$, and to match with the normal state, $2\alpha = \chi_n(T)^{-1}$ is the inverse normal-state magnetic susceptibility. At zero magnetic field the magnetization associated with the order parameter can be shown to stabilize the nonunitary state [1]. However, in the presence of magnetic field, and particularly in the vortex state, the resulting magnetization should reflect a competition between the normal-state component and the superconducting tendency to screen the nucleation of a finite magnetization. Here, we present a simple analysis of the electromagnetic response of a strongly paramagnetic superconductor, which seems to account for the experimental results that demonstrate the effect of screening in strongly reducing the magnetization as the temperature tends to zero.

II. EXPERIMENT

To study the interplay between time-reversal symmetry breaking (TRSB) in the superconducting state of UTe_2 and the vortex state, we performed high-resolution polar Kerr effects (PKEs) using a zero-area Sagnac interferometer (ZASI) that probes the sample at a wavelength of 1550 nm, in a He-3 cryostat with base temperature $\lesssim 0.3$ mK. The UTe_2 single crystal used in this study and a basic schematic of the low-temperature setup are shown in Fig. 1, while the full apparatus is described in the Supplemental Material (SM) [17].

In general, the Kerr effect is defined through an asymmetry of reflection amplitudes of right- and left-circularly polarized light from a given material, yielding a Kerr rotation angle θ_K , and is observed only if reciprocity is broken. Thus, in the absence of any time dependence or irreversible effects, a finite Kerr effect unambiguously points to TRSB

in that material system. From its nature, the Kerr effect is described within the general theory of scattering, and thus it is ideal to probe TRSB in superconductors since it is not subjected to shielding (Meissner) effects that counter the magnetization. However, restrictions on the possible observation of a finite Kerr effect suggest that for pure crystals, measurements at frequencies where interband pairing effects are important yield a maximum signal, although still very small [18–21].

In the Kerr measurements reported here we use a collimated beam of diameter $\sim 10.6 \mu\text{m}$, which emerges from a lens and quarter-wave plate assembly that were designed to minimize sensitivity to changes in both angle and distance relative to the sample so as to prevent temperature-dependent changes in optical alignment [22]. For all the measurements the beam is aimed at the center of the sample of average diameter 1.2 mm. However, probing the system at near-infrared frequencies ω , which is much larger than the superconducting gap energy Δ , will reduce a typical ferromagneticlike response of order ~ 1 rad by a factor of $(\Delta/\hbar\omega)^2 \sim 10^{-7}$, yielding a theoretically predicted signal of about 0.1–1 μrad . Thus a sensitive device is needed to detect such small signals, and the ZASI with its high degree of common-mode rejection for any reciprocal effects (e.g., linear birefringence, optical activity, etc.) is probably the most suitable one for this study.

In a typical FC Kerr experiment of a weak-pinning superconductor, the sample is first cooled in a field (FC) lower than $H_{c1}(0)$. The Kerr effect is then measured at zero field while warming up (ZFW). In this case the ZFW measurement yields results similar to the largest Kerr value obtained in a zero-field cool (ZFC) followed by ZFW experiment, indicating a single-domain Kerr response. If the sample is cooled in a field larger than $H_{c1}(0)$, some flux will be trapped after removing the magnetic field at low temperatures, which, depending on the magnetic susceptibility of the material, may result in a finite Kerr effect. Determining the magnetic contribution above T_c , we expect that upon cooling in a field $H_{c1} \lesssim H \ll H_{c2}$, a normal-state contribution will be smaller by at least a factor H/H_{c2} . Thus, without explicit magnetism (that is, magnetic response beyond Pauli paramagnetism or Landau diamagnetism), such effects are undetectable. Indeed, in previous Kerr measurements of Sr_2RuO_4 [23], where a Kerr effect of $\sim 0.1 \mu\text{rad}$ was detected, or the heavy-fermion uranium-based superconductors UPt_3 [24] and URu_2Si_2 [25], and the filled skutterudite $\text{PrOs}_4\text{Sb}_{12}$ [26] (giving a larger signal of ~ 0.4 – $0.7 \mu\text{rad}$, which is expected due to their strong spin-orbit interaction), the same magnitude of Kerr effect was observed irrespective of the magnitude of the orienting FC. Testing the apparatus with reciprocal reflecting media such as simple BCS superconductors (or just mirrors), as well as the spin-singlet d -wave heavy-fermion compound CeCoIn_5 , yielded a null result as expected [27].

Note that unless otherwise indicated, all temperature dependence data were averaged over temperature bins of 100 mK. Error bars in all the plotted data correspond to one standard deviation of the respective statistical average. Low-field studies use oersteds as the magnetic field units where 1 Oe = 1000/4 π A/m.

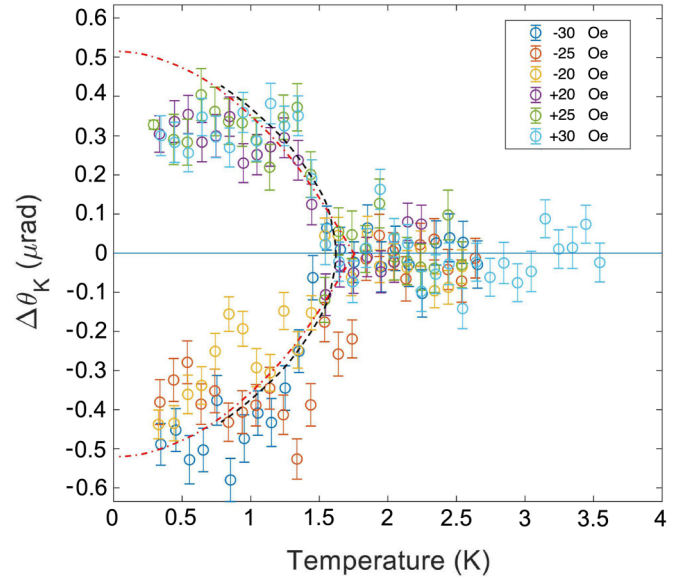


FIG. 2. Very low field cool: Measurements at zero-field warmup. Note that the saturated Kerr angle is the same for this field range. Here, the dash-dotted line (red) is a fit to $[1 - (T/T_c)^2]$ with $T_c = 1.7$ K, while the dashed line (black) is a fit to $[1 - (T/T_c)]^{1/2}$ with $T_c = 1.55$ K, which should dominate near the actual TRSB temperature.

III. RESULTS

Zero-field data. Polar Kerr effect measurements were performed at low temperatures on a single crystal of UTe_2 , after first cooling it to a base temperature of 0.3 K in an ambient field of ~ 0.2 Oe (which we will denote as zero field) and measuring while warming the sample to above the superconducting transition of $T_c \approx 1.55$ K. The cumulative results of five cooldowns are shown in Fig. 1(c) and are consistent with measurements on a second crystal. We note that different cooldowns result in a random size and random sign of the signal, bound by a maximum signal of $|\theta_K| \approx 0.4 \mu\text{rad}$ at 0.3 K. While these zero-field-cool data may point to domain formation, it is typically assumed that with a two-state order parameter, as we anticipate in UTe_2 , domains may be costly; thus often measurements will result in the full signal.

Low-field data. Assuming that the zero-field data arise from the TRSB order parameter, we use field-cool data, with the field oriented along the c direction of the crystal, to test for the ability to couple to that order parameter and at the same time orient the sample to a single domain. This is a crucial part of the correct determination of the possible components of the proposed nonunitary order parameter [1].

First we note that for FC measurements of $H \lesssim 15$ Oe we see no difference from ZFC experiments; that is, values can fluctuate in each cooldown similar to Fig. 1. Figure 2 shows a set of six different experiments where the sample was cooled in magnetic fields of ± 20 , ± 25 , and ± 30 Oe, and the Kerr angle was measured in a ZFW configuration. The low-temperature Kerr angle of this collection of data seems to saturate at the same value, which also coincides with the maximum value obtained in the ZFC experiments. We therefore conclude that this value of $\theta_K \approx 0.4 \mu\text{rad}$ is the intrinsic

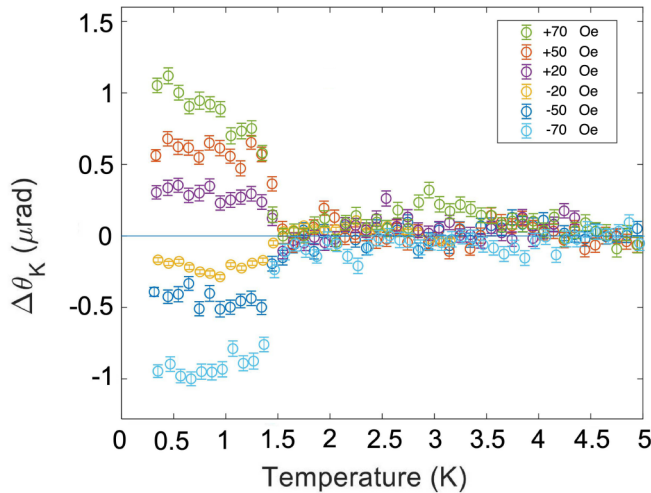


FIG. 3. Low-field cool. Note increase in Kerr signal as $H \geq 50$ Oe.

contribution due to the TRSB order parameter. Attempting to fit the temperature behavior to the standard form of an order parameter $\propto [1 - (T/T_c)^2]$ yields a reasonable fit, but with a slightly higher T_c than where the Kerr effect seems to vanish. A better fit $\propto [1 - (T/T_c)]^{1/2}$ with the actual T_c seems to hold near where the Kerr effect vanishes, thus indicating the existence of a composite order parameter. However, below $\sim T_c/2$, $\theta_K(T)$ develops an anomalous behavior, exhibiting a flatter temperature dependence. Such a behavior may be a precursor to a more pronounced flat temperature behavior that we observe upon cooling in higher magnetic fields, and is typical for the remanent magnetization behavior of a “hard superconductor,” which exhibits large vortex critical current [14,28]. Its occurrence in UTe_2 is a central theme of this paper.

Increasing the training magnetic field above ~ 30 Oe, Fig. 3 shows that the low-temperature Kerr angle saturation value now increases with field, and continues to show a rather flat behavior in approaching T_c , thus further supporting our hypothesis that the Kerr response through $\sigma_{xy}(\omega)$ originates from the intrinsic magnetism. However, the increase in remanent Kerr value indicates that the vortex state induced by the external cooling field now dominates, which is observed through the interaction with the induced magnetism.

Wider field range. When further increasing the magnetic field, a closer resemblance to the behavior of the magnetization of a strong-pinning superconductor in the critical state is revealed. For example, inspection of remanent magnetization in field-cool measurements on URu_2Si_2 and UPt_3 [29] shows an evolution very similar to that of our Kerr measurements in Fig. 3 and the subsequent increased field regime shown in Fig. 4. At the same time, we notice that in our previous measurements of the Kerr effect in these materials the TRSB Kerr signal was independent of the training field [24,25], thus corroborating the claim that the Kerr effect in these materials directly detects the TRSB order parameter.

Measurements in finite magnetic field. The conclusion in Ref. [1] that the order parameter is nonunitary with ($\psi_1 \in B_{3u}$, $\psi_2 \in B_{2u}$), which is stabilized by magnetic fluctuations,

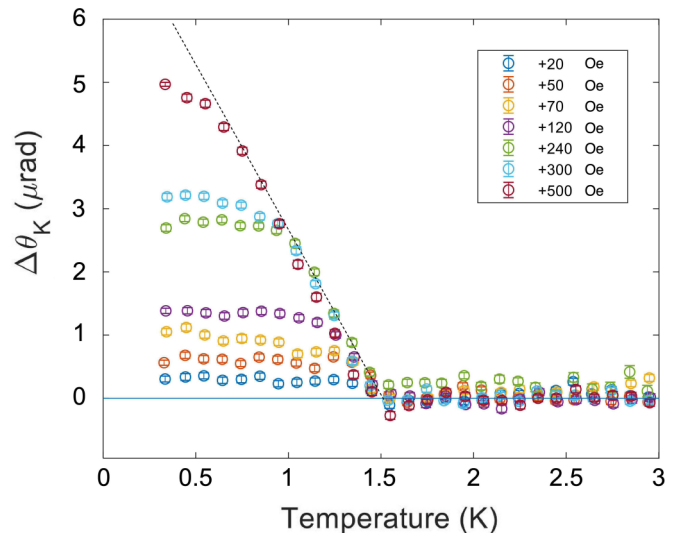


FIG. 4. Temperature dependence remanent Kerr effect after field cool. The dashed line denotes the “envelope” behavior as the cooling field is increased. It extrapolates to $\Delta\theta_K \approx 8.0 \mu\text{rad}$, which would correspond to an approximate cooling field of ~ 920 Oe using extrapolation of the fit shown in Fig. 6.

suggests the possibility that in the presence of magnetic field the composite order parameter may appear at a higher temperature, either at the higher T_c or as a fluctuation-induced effect [30]. Assuming a standard correspondence between the Kerr and magnetization measurements (see, e.g., Ref. [31]), Fig. 5 shows a comparison of the Kerr effect measurement below 16 K and superconducting quantum interference device (SQUID) magnetometry of a similar sample from the same batch. Measurements were done at 240 Oe along the c axis and are plotted relative to the Kerr effect at 16 K (below ~ 1000 Oe the magnetic susceptibility is roughly field independent, possibly exhibiting a weak minimum at ~ 240 Oe; see SM [17]). Also marked in Fig. 5 is the T_c as determined from Fig. 3. While there is a good correspondence between the Kerr response and the magnetization, an anomaly in the Kerr effect is detected in the range of 2 K to ~ 6 K, which could be traced to the interplay between the magnetization along different axes in that regime (see SM [17]). Note further that in the same temperature regime (from T_c to ~ 5 K), muon-spin relaxation studies [8] observed a continuous slowing down of magnetic fluctuations, which they assigned to weak ferromagnetic fluctuations typically observed when a magnetic instability is approached.

IV. ANALYSIS AND DISCUSSION

Magneto-optical effects are described within quantum theory as the interaction of photons with electron spins through spin-orbit interaction (see, e.g., Ref. [32]). In a ferromagnetic material the Kerr angle is found to scale with the magnetization [33], while inherently antiferromagnetic systems may still exhibit a finite Kerr effect depending on their local symmetry (see, e.g., Ref. [34]).

Focusing on the measurements on UTe_2 , we first note that for all FC measurements of $H \lesssim 15$ Oe, including ZFC,

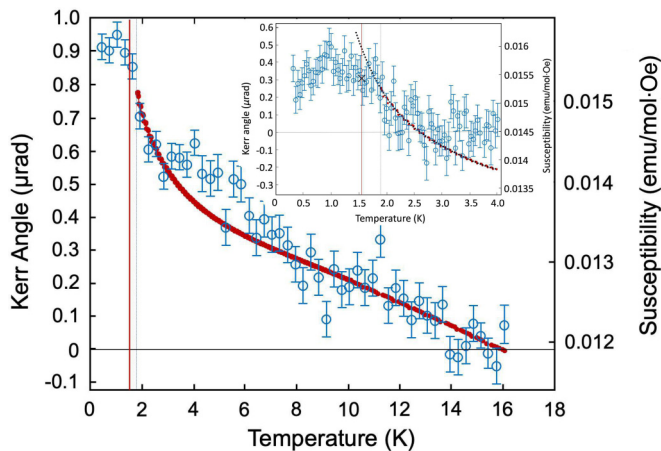


FIG. 5. Susceptibility and Kerr effect measurements of UTe_2 in magnetic fields below H^* . For the Kerr effect the sample was cooled in a magnetic field of 240 Oe and then measured when warmed up in 240 Oe (Kerr data points represent a bin average of 0.3 K and are plotted relative to the Kerr angle at 16 K). Susceptibility data were measured in a SQUID magnetometer down to 1.8 K and were fitted to the Kerr data in the temperature range of 7–8 K assuming $\theta_K \propto \chi = M/H$. The vertical red line is the zero-field warmup T_c . The inset shows an expanded vertical scale and 100-mK bin average, where the Kerr angle was offset to the plateau around 4 K. The dotted line is the extrapolation of the SQUID-measured susceptibility shown in the main panel fitted below 4 K to the lowest susceptibility temperature measurement of 1.8 K (represented with a faint vertical line). The vertical red line is the zero-field warmup $T_c = 1.55$ K, which meets the local averaged Kerr data at the \times symbol.

the sample exhibits a random-in-sign-and-in-magnitude Kerr signal, which is bound by $|\theta_K(0)| \approx 0.4 \mu\text{rad}$. This clearly establishes an intrinsic TRSB associated with the superconducting order parameter rather than a mere magnetic response. However, as will be discussed below, UTe_2 is a strong-pinning superconductor, clearly exhibiting critical-state features, which will require further considerations in analyzing the low-field data.

Low-field data. The fact that no field dependence is observed for ZFW measurements that follow either ZFC or FC of $H \lesssim 30$ Oe suggests that this very low field effect is a result of either the TRSB order parameter or a constant remanent magnetization, which is induced by an internal ordering field rather than the external cooling field. This may occur if the cooling field H aligns the order parameter $\vec{\psi}$, which in turn induces a finite magnetization through the bilinear coupling term as in Eq. (1). Indeed, Paulsen *et al.* [13] reported that expulsion of flux in FC experiments was negligible in fields greater than just a few gauss. Such bulk magnetization measurements may reflect a critical state that persists even below H_{c1} [28,35]. By contrast, in our Kerr measurements the $\sim 10.6\text{-}\mu\text{m}$ -diameter beam points at the center of a sample of average diameter 1.2 mm [see Fig. 1(b)]. Thus, in such measurements along the applied magnetic fields, we expect the center of the sample to be practically vortex free (in the pure sense of the critical-state model it is completely vortex free).

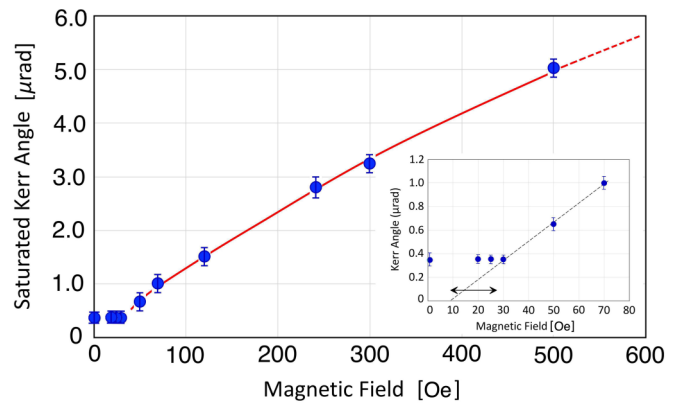


FIG. 6. Saturated Kerr angle vs field in UTe_2 .

Flux pinning, the critical state, and high-field data. UTe_2 is a strongly paramagnetic material, with large magnetic susceptibility above the superconducting T_c . Further observations of strong magnetic hysteresis, a weak Meissner effect, and a large critical current [13] imply the presence of a critical state [14], where cooling in a magnetic field may result in large remanent magnetization. While this may impact field-cool Kerr measurements, the configuration of the experiment may also provide new insight into the critical-state phenomenon in this material. Moreover, it was shown by Clem and Hao [28] that with strong pinning, even below $H_{c1}(0)$, cooling in a field results in remanent magnetization that is only weakly temperature dependent when warming up, and disappears only above the irreversibility temperature $T_{irr} < T_c$ [29]. Increasing further the magnetic field will result in an increase in the remanent magnetization, until a field $H^*(T)$ is reached, where for a given temperature T , full flux penetration into the center of the sample occurs. Assuming that in this field regime the Kerr angle is proportional to the remanent magnetization in the material, we first extrapolate the envelope of the temperature dependence of the $\theta_K(T)$ to $T = 0$, obtaining an extrapolated value of $8.0 \pm 0.3 \mu\text{rad}$. Next we plot the saturated Kerr angle from Fig. 4 as a function of cooling field as shown in Fig. 6. Combining these two measurements, we find that the Kerr angle at $T = 0$ will be maximum in a field cool of $H_{\text{max}} \approx 920$ Oe. Since we assume that the vortex state, which induces the finite magnetization, is in the critical state, the vortex distribution in space is determined by the critical current, which is assumed constant [15]. In this model the vortex-density profile [i.e., the profile of the magnetic induction $B(r)$] is a straight line, matching the external field at the sample surface. If the external field is taken to zero before warming up, this profile determines the variation of the remanent magnetization in space. Obviously, with the above approximation the maximum remanent magnetization is obtained for a magnetic field H^* for which a first vortex is introduced to the center of the sample. Similarly, we will need to take the external magnetic field to $-H^*$ to subsequently have the center of the sample completely screened. For a sample of averaged diameter D , the above arguments imply

$$H^* = \frac{2\pi J_c D}{c} \quad \text{or} \quad J_c = \frac{c}{2\pi D} H^*. \quad (2)$$

Taking for our data $H^* \approx H_{\max} = 920$ Oe, we obtain $J_c \approx 1.05 \times 10^4$ A/cm², which is very close to the critical currents recently measured for UTe₂ of $J_c^a \approx 0.8 \times 10^4$ A/cm² and $J_c^b \approx 1.6 \times 10^4$ A/cm² [13]. This agreement between the Kerr data and the direct measurements of the critical current further support our interpretation of the origin of the Kerr signal above H_{c1} .

Further support of the critical-state scenario is discussed in the SM [17], where we analyze a hysteresis loop at a field much smaller than H^* , demonstrating how the evolution of the superconducting order counteracts the increase in magnetization below T_c . While cooling in a field nucleates remanent magnetization, cooling at zero field and increasing the field to $H_{c1} \ll H < H^*$ results in a weak Kerr effect at the center of the sample, which is further reduced almost completely as the field is reduced to zero.

It is important to note the difference between UTe₂ and other uranium-based superconductors that exhibit a critical state. Focusing on UPt₃ and URu₂Si₂, Kozioł *et al.* [29] show remanent magnetization curves for these two materials for field below their respective H^* . At the same time, our own Kerr measurements on these materials [24,25] show that the Kerr effect in FC measurements is independent of cooling field and it coincides with the envelope of the zero-field-cool experiments. The reason is, as explained above, that with no explicit magnetism, the trapped vortices only carry a Kerr effect due to Pauli paramagnetism or Landau diamagnetism, which is reduced by those vortices' relative density of H/H_{c2} . Such an effect is undetectable with our resolution of nanoradians. At the same time, the Kerr measurements on UTe₂ do resemble the bulk magnetization measurements of UPt₃ and URu₂Si₂ [29] (see SM [17]). This clearly indicates that the cores of the vortices in UTe₂ are magnetized, with the magnetization aligned with the direction of the cooling field. This retention of the full magnetization upon the removal of the magnetic field (see SM [17]) further suggests a proximity to a ferromagnetic transition as also concluded by the muon-spin relaxation on similar samples [8].

TRSB order parameter in magnetic field. From inspection of Fig. 5, the normal-state (FW) Kerr data show a standard increase consistent with a paramagnetic susceptibility of the material, before experiencing a sharp increase below ~ 6 K which seems to return to the original susceptibility curve below ~ 2 K. Indeed, a change in course of the magnetic susceptibility was previously noted in this temperature range by several groups [36,37], typically attributed to the c direction being perpendicular to the easy axis a (see also SM [17]). To better understand the observed behavior, we show in the inset of Fig. 5 the expanded data below 4 K (data points represent a bin average of 100 mK), which include the superconducting transition region. Since susceptibility data are only available down to 1.8 K, our analysis needs to rely on the extrapolation of these normal-state data to lower temperatures; however, inspection of the trend of the data already suggests that the extrapolated susceptibility will go above the average of the Kerr angle at T_c , marked with the cross (\times) symbol at the T_c of the ZFW measurements (e.g., Fig. 4). To illustrate this claim, we fit the susceptibility data below 4 K (a fourth-order polynomial gives the best fit) and extrapolate it lower than the measured 1.8 K. The extrapolated susceptibility, which

represents the normal-state magnetic response, clearly overshoots above the actual Kerr data. This behavior may indicate the emergence of superconducting fluctuations, which are expected to compete with the magnetic fluctuations already above T_c .

Since our experiment does not detect the Meissner currents that shield the whole crystal, the data must indicate the competition between the paramagnetic susceptibility and the superconducting order parameter that develops in the interior of the sample. This in turn suggests that the proximity to the superconducting state is felt already ~ 0.3 K above the Kerr-detected T_c . However, as T_c is approached, the magnetic response weakens, and the Kerr angle at the center of the sample decreases towards its value at T_c . Such an effect cannot be described by Eq. (1), which considers a uniform magnetic field and ignores screening effects. Instead, to understand this effect, we need to include the full electrodynamics of the superconductor and its interaction with the magnetization. Since the Kerr effect is expected to follow the magnetization, including the TRSB effect of the superconducting order parameter, we revise Eq. (1), writing

$$f_m = \alpha m^2 + c|\nabla m|^2 + \gamma m\tilde{\psi} - mh, \quad (3)$$

where we added a term that allows for nonuniform magnetization, which is expected in the vortex state, and the external magnetic field is replaced with the local magnetic field $\vec{h}(\vec{r})$, which we will take as pointing in the c direction (thus we omit the vector sign). This local field arises from the solution of the Ginzburg-Landau equations, and thus its profile through the vortices already includes the field penetrating through the core and the shielding currents that extend a penetration-depth distance λ beyond the vortex core. Moreover, we recall that $\langle \vec{h}(\vec{r}) \rangle = \vec{B}$, the magnetic induction of the superconductor. A more detailed approach, aimed at analyzing the magnetic structure in a ferromagnetic superconductor, was recently presented by Devizorova *et al.* [38]. However, here we were only interested in the magnitude of the average magnetization. Thus, to obtain the equilibrium contribution of the paramagnetism to the magnetization in the superconductor, we minimize the magnetic free energy with respect to m , obtaining

$$\frac{1}{\chi_n} [1 - a^2 \nabla^2] m = h - \gamma \tilde{\psi}, \quad (4)$$

where, as in Eq. (1), we identify $2\alpha = \chi_n(T)^{-1}$ as the inverse of the normal-state magnetic susceptibility and $a^2 = c/\alpha$ is the magnetic stiffness parameter, which represents a microscopic length of order lattice constant. Now, $(h - \gamma \tilde{\psi})$ acts as an effective local magnetic field that follows the vortex lattice periodicity. As we solve for the magnetization and substitute back in Eq. (3), we clearly observe that the large magnetic susceptibility caused by magnetic fluctuations further enhances the effective field $\sim \chi h$ that couples to the composite order parameter. Taking the Fourier transform of Eq. (4), we arrive at the q component of the transform for the magnetization:

$$m_q = \chi_n \frac{h_q - \gamma \tilde{\psi}_q}{1 + a^2 q^2}. \quad (5)$$

However, since h_q arises from the London equation, it should decay with the penetration length λ away from the vortex center; thus $h_q = h(0)/(1 + \lambda^2 q^2)$. We thus expect

$$m_q = \frac{\chi_n}{1 + a^2 q^2} \frac{h(0) - \gamma \langle \tilde{\psi} \rangle}{1 + \lambda^2 q^2}. \quad (6)$$

The total magnetization density is then

$$\langle m \rangle = \sum_q \frac{\chi_n}{1 + a^2 q^2} \frac{B - \gamma \langle \tilde{\psi} \rangle}{1 + \lambda^2 q^2}. \quad (7)$$

Near T_c the sum is dominated by $q \rightarrow 0$, yielding the same result we would expect from Eq. (1), that is,

$$\langle m \rangle_{T \approx T_c} = \chi_n (B - \gamma \langle \tilde{\psi} \rangle). \quad (8)$$

However, as the temperature tends towards zero, we cannot ignore the shorter wavelengths, which will be dominated by the vortex lattice wave vector, $q \approx \sqrt{\Phi_0/B}$. Since in that regime $a^2 B/\Phi_0 \ll 1$, while $\lambda^2 B/\Phi_0 \approx B/H_{c1} \gg 1$, we can change the sum to an integral, and [up to order of $\ln(\lambda/\xi)$, where ξ is the superconducting coherence length], we obtain

$$\langle m \rangle_{T \ll T_c} \approx \chi_n \frac{H_{c1}}{B} (B - \gamma \langle \tilde{\psi} \rangle), \quad (9)$$

which demonstrates the effect of screening. Here, $\chi_n(T) \rightarrow \infty$ as $T \rightarrow 0$, before saturating to its full value at $T = 0$. Thus without the large reduction of H_{c1}/B , the magnetization would monotonically increase towards zero temperature. Our experimental data for the Kerr effect at 240 Oe, which is much larger than H_{c1} , indeed agree with the trend calculated above. This unique behavior is clearly demonstrated in Fig. 5.

V. CONCLUSIONS

UTe₂ exhibits strong paramagnetic fluctuations, with no apparent finite-temperature magnetic order. Using the magneto-optic polar Kerr effect to study the magnetic behavior of UTe₂ crystals, while focusing our detection beams

on the center of the sample, away from any surface Meissner currents, we are able to study the pure superconducting wave-function response at very low field and the evolution of the vortex critical state at higher field. This approach allows for a clear demonstration of the properties of a critical state that appears in this material in the presence of an applied magnetic field, including the determination of the critical current density for vortex motion when the field is applied in the c direction. When vortices are present, a finite magnetization is detected, confirming the proximity to a magnetic critical point, possibly a quantum critical one. Subtracting out the magnetic effect, the order parameter shows an orbital TRSB effect of size similar to the B phase of UPt₃ [24] and the low-temperature behavior of the superconducting state of URu₂Si₂ [25]. Finally, measurements in the presence of magnetic field clearly show the tendency of the superconductor to produce shielding currents that oppose the increase in vortex-induced magnetization due to the diverging paramagnetic susceptibility.

ACKNOWLEDGMENTS

We acknowledge discussions with Steve Kivelson and Ronny Thomale. Work at Stanford University was supported by the Department of Energy, Office of Basic Energy Sciences, under Contract No. DE-AC02-76SF00515. Work at University of Wisconsin was supported by the Department of Energy, Office of Basic Energy Sciences, Division of Materials Sciences and Engineering, under Award No. DE-SC0021971. Research at the University of Maryland was supported by Air Force Office of Scientific Research Award No. FA9550-14-1-0332, Department of Energy Award No. DE-SC-0019154 (specific heat experiments), the Gordon and Betty Moore Foundation's EPiQS Initiative through Grant No. GBMF9071 (materials synthesis), NIST, and the Maryland Quantum Materials Center. Sample synthesis and preliminary characterization were supported by NIST. Work at Karlsruhe was supported by Deutsche Forschungsgemeinschaft (German Research Foundation) Project No. ER 463/14-1.

-
- [1] I. M. Hayes, D. S. Wei, T. Metz, J. Zhang, Y. S. Eo, S. Ran, S. R. Saha, J. Collini, N. P. Butch, D. F. Agterberg, A. Kapitulnik, and J. Paglione, Multicomponent superconducting order parameter in UTe₂, *Science* **373**, 797 (2021).
- [2] A. H. Nevidomskyy, Stability of a nonunitary triplet pairing on the border of magnetism in UTe₂, [arXiv:2001.02699](https://arxiv.org/abs/2001.02699) [cond-mat.supr-con].
- [3] T. Shishidou, H. G. Suh, P. M. R. Brydon, M. Weinert, and D. F. Agterberg, Topological band and superconductivity in UTe₂, *Phys. Rev. B* **103**, 104504 (2021).
- [4] L. P. Cairns, C. R. Stevens, C. D. O'Neill, and A. Huxley, Composition dependence of the superconducting properties of UTe₂, *J. Phys.: Condens. Matter* **32**, 415602 (2020).
- [5] S. M. Thomas, C. Stevens, F. B. Santos, S. S. Fender, E. D. Bauer, F. Ronning, J. D. Thompson, A. Huxley, and P. F. S. Rosa, Spatially inhomogeneous superconductivity in UTe₂, *Phys. Rev. B* **104**, 224501 (2021).
- [6] Y. Tokunaga, H. Sakai, S. Kambe, T. Hattori, N. Higa, G. Nakamine, S. Kitagawa, K. Ishida, A. Nakamura, Y. Shimizu, Y. Homma, D. Li, F. Honda, and D. Aoki, ¹²⁵Te-NMR study on a single crystal of heavy fermion superconductor UTe₂, *J. Phys. Soc. Jpn.* **88**, 073701 (2019).
- [7] G. Nakamine, K. Kinjo, S. Kitagawa, K. Ishida, Y. Tokunaga, H. Sakai, S. Kambe, A. Nakamura, Y. Shimizu, Y. Homma, D. Li, F. Honda, and D. Aoki, Anisotropic response of spin susceptibility in the superconducting state of UTe₂ probed with ¹²⁵Te-NMR measurement, *Phys. Rev. B* **103**, L100503 (2021).
- [8] S. Sundar, S. Gheidi, K. Akintola, A. M. Côté, S. R. Dunsiger, S. Ran, N. P. Butch, S. R. Saha, J. Paglione, and J. E. Sonier, Coexistence of ferromagnetic fluctuations and superconductivity in the actinide superconductor UTe₂, *Phys. Rev. B* **100**, 140502(R) (2019).

- [9] T. R. Kirkpatrick and D. Belitz, Exponent relations at quantum phase transitions with applications to metallic quantum ferromagnets, *Phys. Rev. B* **91**, 214407 (2015).
- [10] C. Duan, K. Sasmal, M. B. Maple, A. Podlesnyak, J.-X. Zhu, Q. Si, and P. Dai, Incommensurate Spin Fluctuations in the Spin-Triplet Superconductor Candidate UTe_2 , *Phys. Rev. Lett.* **125**, 237003 (2020).
- [11] W. Knafo, G. Knebel, P. Steffens, K. Kaneko, A. Rosuel, J.-P. Brison, J. Flouquet, D. Aoki, G. Lapertot, and S. Raymond, Low-dimensional antiferromagnetic fluctuations in the heavy-fermion paramagnetic ladder compound UTe_2 , *Phys. Rev. B* **104**, L100409 (2021).
- [12] S. M. Thomas, F. B. Santos, M. H. Christensen, T. Asaba, F. Ronning, J. D. Thompson, E. D. Bauer, R. M. Fernandes, G. Fabbris, and P. F. S. Rosa, Evidence for a pressure-induced antiferromagnetic quantum critical point in intermediate-valence UTe_2 , *Sci. Adv.* **6**, eabc8709 (2020).
- [13] C. Paulsen, G. Knebel, G. Lapertot, D. Braithwaite, A. Pourret, D. Aoki, F. Hardy, J. Flouquet, and J.-P. Brison, Anomalous anisotropy of the lower critical field and Meissner effect in UTe_2 , *Phys. Rev. B* **103**, L180501 (2021).
- [14] J. R. Clem, Theory of ac losses in type-II superconductors with a field-dependent surface barrier, *J. Appl. Phys. (Melville, NY)* **50**, 3518 (1979).
- [15] C. P. Bean, Magnetization of Hard Superconductors, *Phys. Rev. Lett.* **8**, 250 (1962).
- [16] C. P. Bean, Magnetization of high-field superconductors, *Rev. Mod. Phys.* **36**, 31 (1964).
- [17] See Supplemental Material at <http://link.aps.org/supplemental/10.1103/PhysRevB.105.024521> for details on the device characterization and data analysis (includes Refs. [39,40]).
- [18] K. I. Wysokiński, J. F. Annett, and B. L. Györfy, Intrinsic Optical Dichroism in the Chiral Superconducting State of Sr_2RuO_4 , *Phys. Rev. Lett.* **108**, 077004 (2012).
- [19] E. Taylor and C. Kallin, Intrinsic Hall Effect in a Multiband Chiral Superconductor in the Absence of an External Magnetic Field, *Phys. Rev. Lett.* **108**, 157001 (2012).
- [20] M. Gradhand, K. I. Wysokiński, J. F. Annett, and B. L. Györfy, Kerr rotation in the unconventional superconductor Sr_2RuO_4 , *Phys. Rev. B* **88**, 094504 (2013).
- [21] C. Kallin and J. Berlinsky, Chiral superconductors, *Rep. Prog. Phys.* **79**, 054502 (2016).
- [22] E. R. Schemm, Optical characterization of time reversal symmetry breaking states in heavy fermion superconductors, Ph.D. thesis, Stanford University, 2014.
- [23] J. Xia, P. T. Beyersdorf, M. M. Fejer, and A. Kapitulnik, Modified Sagnac interferometer for high-sensitivity magneto-optic measurements at cryogenic temperatures, *Appl. Phys. Lett.* **89**, 062508 (2006).
- [24] E. R. Schemm, W. J. Gannon, C. M. Wishne, W. P. Halperin, and A. Kapitulnik, Observation of broken time-reversal symmetry in the heavy-fermion superconductor UPt_3 , *Science* **345**, 190 (2014).
- [25] E. R. Schemm, R. E. Baumbach, P. H. Tobash, F. Ronning, E. D. Bauer, and A. Kapitulnik, Evidence for broken time-reversal symmetry in the superconducting phase of URu_2Si_2 , *Phys. Rev. B* **91**, 140506(R) (2015).
- [26] E. M. Levenson-Falk, E. R. Schemm, Y. Aoki, M. B. Maple, and A. Kapitulnik, Polar Kerr Effect from Time-Reversal Symmetry Breaking in the Heavy-Fermion Superconductor $PrOs_4Sb_{12}$, *Phys. Rev. Lett.* **120**, 187004 (2018).
- [27] E. Schemm, E. Levenson-Falk, and A. Kapitulnik, Polar Kerr effect studies of time reversal symmetry breaking states in heavy fermion superconductors, *Phys. C (Amsterdam)* **535**, 13 (2017).
- [28] J. R. Clem and Z. Hao, Theory for the hysteretic properties of the low-field dc magnetization in type-II superconductors, *Phys. Rev. B* **48**, 13774 (1993).
- [29] Z. Kozioł, J. J. M. Franse, P. F. de Châtel, and A. A. Menovsky, Magnetization of a superconductor: Results from the critical-state model, *Phys. Rev. B* **50**, 15978 (1994).
- [30] J. Schmalian, Notes on superconductivity in UTe_2 (private communication).
- [31] J. Xia, W. Siemons, G. Koster, M. R. Beasley, and A. Kapitulnik, Critical thickness for itinerant ferromagnetism in ultrathin films of $SrRuO_3$, *Phys. Rev. B* **79**, 140407(R) (2009).
- [32] P. S. Pershan, Magneto-optical effects, *J. Appl. Phys. (Melville, NY)* **38**, 1482 (1967).
- [33] P. N. Argyres, Theory of the Faraday and Kerr effects in ferromagnetics, *Phys. Rev.* **97**, 334 (1955).
- [34] J. Orenstein, Optical Nonreciprocity in Magnetic Structures Related to High- T_c Superconductors, *Phys. Rev. Lett.* **107**, 067002 (2011).
- [35] L. Krusin-Elbaum, A. P. Malozemoff, D. C. Cronmeyer, F. Holtzberg, J. R. Clem, and Z. Hao, New mechanisms for irreversibility in high- T_c superconductors (invited), *J. Appl. Phys. (Melville, NY)* **67**, 4670 (1990).
- [36] S. Ran, C. Eckberg, Q.-P. Ding, Y. Furukawa, T. Metz, S. R. Saha, I.-L. Liu, M. Zic, H. Kim, J. Paglione, and N. P. Butch, Nearly ferromagnetic spin-triplet superconductivity, *Science* **365**, 684 (2019).
- [37] S. Ikeda, H. Sakai, D. Aoki, Y. Homma, E. Yamamoto, A. Nakamura, Y. Shiokawa, Y. Haga, and Y. Ōnuki, Single crystal growth and magnetic properties of UTe_2 , *J. Phys. Soc. Jpn.* **75**, 116 (2006).
- [38] Z. Devizorova, S. Mironov, and A. Buzdin, Theory of Magnetic Domain Phases in Ferromagnetic Superconductors, *Phys. Rev. Lett.* **122**, 117002 (2019).
- [39] V. Hutanu, H. Deng, S. Ran, W. T. Fuhrman, H. Thoma, and N. P. Butch, Low-temperature crystal structure of the unconventional spin-triplet superconductor UTe_2 from single-crystal neutron diffraction, *Acta Crystallogr. Sect. B: Struct. Sci. Cryst. Eng. Mater.* **76**, 137 (2020).
- [40] S. Bae, H. Kim, Y. S. Eo, S. Ran, I.-L. Liu, W. T. Fuhrman, J. Paglione, N. P. Butch, and S. M. Anlage, Anomalous normal fluid response in a chiral superconductor UTe_2 , *Nat. Commun.* **12**, 2644 (2021).